This article has been accepted for publication in a future issue of this journal, but has not been fully edited. Content may change prior to final publication. Citation information: DOI 10.1109/JLT.2016.2629081, Journal of Lightwave Technology

Experimental Investigation of All-Optical Relay-Assisted 10 Gbps FSO Link over the Atmospheric Turbulence Channel

Norhanis Aida Mohd Nor, Zabih Ghassemlooy, Jan Bohata, Prakriti Saxena, Matej Komanec, Stanislav Zvanovec, Manav R. Bhatnagar, and Mohammad-Ali Khalighi

***Abstract*— This paper presents novel experimental results for a 10 Gbps triple-hop relay-based all-optical free space optical (FSO) system by employing the amplify-and-forward relaying scheme. We provide a mathematical framework for the end-end signal-to-noise ratio (SNR) and the bit-error rate (BER) performance and confirm that the derived analytical results reasonably match experimental results especially at relatively high SNR. The evaluated BER performances under different atmospheric turbulence regimes (modeled by the Gamma-Gamma distribution) show that the considered relay-assisted FSO system offers a significant performance improvement for weak to strong turbulence regimes, even without knowledge of the channel state information. More precisely, at a target BER of 10^{-5} the proposed scheme offers ~5 dB and ~4 dB of SNR gains compared to the direct transmission for turbulence strengths C_n^2 of 3.8×10^{-10} m$^{-2/3}$ and 5.4×10^{-12} m$^{-2/3}$, respectively.**

***Index Terms*— All-optical relaying, atmospheric turbulence, BER, free space optics (FSO), relay-assisted FSO**

I. Introduction

As third and fourth generations (3G/4G) of mobile networks have experienced tremendous increase of data traffic, the service providers must address the bandwidth bottleneck issues at both the backhaul and last mile access networks in order to increase the network capacity. Both microwave and optical fiber based technologies will continue to retain their importance as a backhaul bearer. However, operators may also consider alternative technologies to overcome the spectrum congestion in certain applications, thus ensuring the most efficient use of the radio frequency (RF) spectrum in dense-traffic areas. This could include point-to-multipoint links in areas where spectrum for the conventional point-to-point links is becoming scarce and costly. To increase bandwidth and capacity, service providers are considering moving to higher frequencies (i.e., 40 and 80 GHz bands), but at the expense of reduced transmission coverage, which has adverse effects on the cost (i.e., deployment, site rental, maintenance, equipment, etc.). Alternatively, the free space optical (FSO) communications-based technology could be adopted to address the aforementioned problems particularly in the last mile access networks at much reduced cost compared to RF based schemes. FSO systems are mostly used for line-of-sight applications, thus offering similar capabilities as optical fiber communications with attractive features including a huge bandwidth, no licensing fee, inherent security, low cost of installation and maintenance, and immunity to electromagnetic interference [1], [2]. Data rates R_d up to 10 Gbps are readily available in commercial FSO systems operating over a link span of few kilometers [3] and up to 1.6 Tbps over a 80 m single outdoor link based on the dense wavelength division multiplexing technique was reported in [4].

Despite these advantages, the FSO link performance is aggravated by the atmospheric phenomena, which are highly variable and unpredictable, such as fog, smoke, clouds, snow, turbulence, and smog, thus resulting in optical attenuation, waveform distortion, and phase wandering due to scattering and absorption [5]. Therefore, with these channel imposed constraints, it is very challenging to attain up to 99.999% link availability [1]. Unlike fog, snow, and cloud, which induce attenuation, the atmospheric turbulence (AT), also known as scintillation, is the main source of random fluctuations of received optical radiation irradiance both in terms of intensity and phase variations even under the clear weather conditions [6]. A number of mitigation techniques have been investigated and proposed to combat the deterioration of signal quality due to adverse aforementioned atmospheric conditions including adaptive optics [7], spatial diversity [8], aperture averaging [9], modulation and signaling formats [10], coding [11], and hybrid RF/FSO systems [12], [13]. However, most of these mitigation techniques have the drawback of incurring high implementation complexity and/or cost. Therefore, with the aim of reducing the complexity and increasing the link span, this paper investigates an alternative approach based on the path routing using the all-optical FSO relay-based system. In this scheme, one or more relay(s) is(are) incorporated to the direct link between the transmitter (Tx) and the receiver (Rx) nodes as illustrated in Fig. 1, which allows reducing path loss

Manuscipt received XX; revised YY; accepted ZZ. Date of publication ZZ1; date of current version ZZ2. This joint research is supported by the EU COST ICT Action IC 1101 and by the Grant Agency of the CTU in Prague, grant no. SGS14/190/OHK3/3T/13. The first author N. A. M. Nor received Ph.D sponsorship from the Ministry of Education Malaysia and she is with the International Islamic University Malaysia, Malaysia. (email: norhanis_aida@iium.edu.my)

N. A. M. Nor and Z. Ghassemlooy are with the Optical Communications Research Group, Faculty of Engineering and Environment, Northumbria University, Newcastle upon Tyne, NE1 8ST, U.K. (e-mail: norhanis.a.m.nor@northumbria.ac.uk; z.ghassemlooy@northumbria.ac.uk).

J. Bohata, M. Komanec, and S. Zvanovec are with the Department of Electromagnetic Field, Faculty of Electrical Engineering, Czech Technical University in Prague, Technicka 2, Prague 16627, Czech Republic (e-mail: bohatja2@fel.cvut.cz; komanmat@fel.cvut.cz; xzvanove@fel.cvut.cz).

P. Saxena and M. R. Bhatnagar are with the Department of Electrical Engineering, Indian Institute of Technology Delhi, Hauz Khas, New Delhi 110016, India (e-mail: prakriti1192@gmail.com; manav@ee.iitd.ac.in).

M.-A. Khalighi is with the École Centrale Marseille, Institut Fresnel, Domaine Universitaire Saint-Jérôme, Marseille 13397, France (e-mail: ali.khalighi@fresnel.fr).

This article has been accepted for publication in a future issue of this journal, but has not been fully edited. Content may change prior to final publication. Citation information: DOI 10.1109/JLT.2016.2629081, Journal of Lightwave Technology

and turbulence per link. Meanwhile, we can benefit from reduced launch power at the Tx and efficient fading reduction at the Rx in the case of employing parallel relays (due to almost independent fading coefficients) [14].

Most theoretical studies reported on relay-assisted FSO systems under turbulence conditions [15]–[18] have considered relay nodes based on electrical-to-optical (EO) and optical-to-electrical (OE) conversion modules. Thus, the need for high-speed electronics and electro-optics devices, analog gain units, and digital control, which contributed to the increased link latency, complexity, and high implementation cost. Alternatively, the entire system could be kept in the optical domain by introducing all-optical relay modules. Analysis of all-optical FSO relay-based systems employing the erbium-doped fiber amplifier (EDFA) based amplify-and-forward (AF) relay were reported in [19]–[22]. In particular, Monte Carlo simulation results for the bit error rate (BER) performance for the FSO relay system using fixed-gain optical amplifiers or optical regenerators under the weak turbulence regime was reported in [20]. In [23], an all-optical AF dual-hop FSO system employing a 4-pulse position modulation operating at the wavelength of 1550 nm over Gamma-Gamma (ΓΓ) turbulence channel was reported showing that the required transmitted power is reduced proportionately to the amplifier gain. For example, with a gain of 10 dB, the transmit power per bit of 10 dBm is conserved at a target BER of 10^{-6} over a link span of 3 km. Furthermore, in [24] a cumulative density function (CDF) analysis for the end-to-end signal-to-noise ratio (SNR) for relay-assisted subcarrier intensity modulation (SIM) all-optical FSO networks over the ΓΓ fading channel considering the pointing error was investigated. The authors also theoretically showed that the improvement in the outage probability can be obtained by employing the multiuser diversity gain. Recently a hybrid RF/FSO was considered to further enhance the system performance by adopting RF and FSO links from source-to-relay and from relay-to-destination, respectively [25], [26]. The authors derived analytical expressions for the probability density function (PDF) and CDF, and investigated the outage probability and the BER performance of a dual-hop relaying system. However, almost all works reported on this topic are theoretical in nature with very little or no experimental verifications.

In [27], we experimentally verified the performance of an all-optical dual-hop 10 Gbps FSO link by employing all-optical switching at the re-transmission point over a turbulence channel. Furthermore, in [28] we numerically simulated the performance of the multi-hop FSO system using a commercial software (with limited tools for turbulence) and showed that there was noticeable improvement in the BER performance compared to the conventional direct single link transmission. We also showed preliminary experimental results for SNR gains of 2.2 dB and 4.7 dB for dual- and triple-hop FSO relay links, respectively, compared to the direct FSO link transmission, [28] at a target BER of 10^{-6} under the turbulence strength of ~10^{-10} $m^{-2/3}$ for a total link span of 6.6 m. In this paper, we significantly extend the experimental investigation campaign previously reported in [27] and [28] for a triple-hop FSO scheme employing AF relaying under different turbulence regimes, governed by ΓΓ distribution. We also outline the mathematical frameworks for the SNR and BER analyses for the proposed scheme supported by experimental validation. We prove that over the entire SNR range, there is an excellent match between the predicted and measured results. We also testify how multi-hop FSO transmission substantially improves the overall link performance under turbulence by exploiting the distance-dependent fading variance of turbulence via implicitly shortening the transmission distance.

The remainder of this paper is organized as follows: Section II provides a brief explanation of the turbulence model and signal transmission formulation. In section III, we present the corresponding FSO performance analysis. Section IV explains the experimental setup. Measured results along with further analyses are discussed in Section V. Lastly, concluding remarks are highlighted in Section VI.

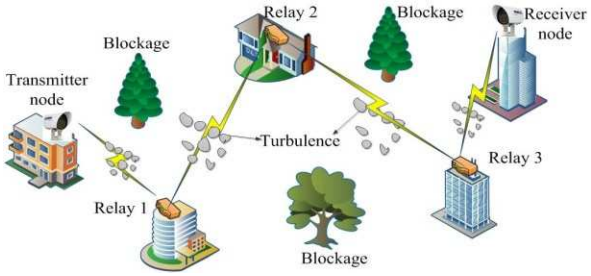

Fig. 1: Illustration of relay-assisted FSO communications

II. System Model

A. Turbulence Model

The turbulence induced fading (TIF), which is one of the main challenges in FSO systems, is due to variation of the refractive index along the propagation path caused especially by inhomogeneities in the temperature and pressure [6]. Due to turbulence eddies the propagating optical beam experiences amplitude and phase fluctuations, and loss of spatial coherence, which can ultimately result in optical power dropping below the Rx threshold level, thus leading to performance deterioration or even a total link failure [29]–[31]. For turbulence induced irradiance fluctuations several statistical models have been proposed [2], [32]. The most common distribution models employed are Log-normal, mainly for weak turbulence, and ΓΓ for weak-to-strong turbulence regimes [33]. In this work, we model the TIF channel between the (j-1)th and jth relay, $h_{j-1,j}$, (indexes 0 and 3 correspond to S and D) by the ΓΓ PDF as given by [6]:

$$\rho_j(h_{j-1,j}) = \frac{2(\alpha\beta)^{(\alpha+\beta)/2}}{\Gamma(\alpha)\Gamma(\beta)} h_{j-1,j}^{\left(\frac{\alpha+\beta}{2}\right)-1} K_{\alpha-\beta}\left(2\sqrt{\alpha\beta h_{j-1,j}}\right), \quad (1)$$

where $\Gamma(\cdot)$ is the Gamma function, $K_{\alpha-\beta}(\cdot)$ is the modified Bessel function of the 2nd kind of order $(\alpha-\beta)$, α and β are the effective numbers of large and small scale eddies of the scattering process, respectively. For the case of plane wave propagation through homogeneous and isotropic atmopsheric turbulence, we have [6]:

$$\alpha = \left[\exp\left(\frac{(0.49\sigma_I^2)}{\left(1+1.11\sigma_I^{12/5}\right)^{7/6}}\right) - 1\right]^{-1}, \quad (2)$$

This article has been accepted for publication in a future issue of this journal, but has not been fully edited. Content may change prior to final publication. Citation information: DOI 10.1109/JLT.2016.2629081, Journal of Lightwave Technology

$$\beta = \left[\exp\left(\frac{(0.51\sigma_I^2)}{\left(1+0.69\sigma_I^{12/5}\right)^{5/6}}\right) - 1\right]^{-1}, \quad (3)$$

where σ_I^2 is the scintillation index, which measures the normalized optical intensity I variance at the Rx as [6]:

$$\sigma_I^2 = \frac{\langle I^2\rangle}{\langle I\rangle^2} - 1, \quad (4)$$

where $\langle\cdot\rangle$ denotes the ensemble average. Note that, in the weak fluctuation regime, σ_I^2 is almost equal to the Rytov variance σ_R^2 [33]. Hence, we have:

$$\sigma_{I,pl}^2 \approx \sigma_R^2 = 1.23 C_n^2 k^{7/6} {d_{j-1,j}}^{11/6}, \quad (5)$$

where $k = \frac{2\pi}{\lambda}$ is the optical wave number, $d_{j-1,j}$ is the propagation distance between (j-1)th and jth relay, and C_n^2 is the refractive index structure parameter that is commonly used to measure the strength of turbulence and is highly dependent on the small scale temperature fluctuations, and the temperature structure constant C_T^2, which is given by [6]:

$$C_n^2 = \left(86 \times 10^{-6} \frac{P}{T^2}\right)^2 C_T^2. \quad (6)$$

Here, P is the atmospheric pressure in millibar and T is the absolute temperature in Kelvin. C_T^2 is related to the universal 2/3 power law of temperature variations as [6]:

$$D_T = \langle (T_1 - T_2)^2 \rangle = \begin{cases} C_T^2 l_o^{-\frac{4}{3}} L_p^2 & \text{for } 0 \ll L_p \ll l_o \\ C_T^2 L_p^{2/3} & \text{for } l_o \ll L_p \ll L_o, \end{cases} \quad (7)$$

where T_1 and T_2 are temperatures at two points separated by the propagation distance L_p, and l_o and L_o are inner and outer scales of the small-temperature fluctuations, respectively [6].

Fig. 2 presents σ_I^2, α, and β as a function of Rytov variance for weak, moderate and strong turbulence regimes and for L_p of 100 m and λ of 1550 nm. Note that, σ_I^2 increases with σ_R^2 reaching the saturation level at σ_R^2 of ~4.5, wheras α decreases in weak turbulence reaching a minimum level at σ_R^2 of ~2.5 and then increasing with σ_R^2 > 2.5. Whereas, β exponentially decreases with σ_R^2 reaching a minimum value determined by the transverse spatial coherence radius of the optical wave [1].

B. Signal Transmission Formulation

As stated previously, we consider here an AF triple-hop FSO system using intensity modulation-direct detection (IM-DD), which consists of four nodes: source (S), relay 1 ($R1$), relay 2 ($R2$), and destination (D), see Fig. 3. We assume that there is no direct link between S and D. At each hop, the relays amplify the received signal and forward it to the next relay or to the destination. We assume that the channels are stationary, memoryless, and ergodic with independent but not necessarily identically distributed fading statistics. The signal $s_0(t)$ is transmitted from S to $R1$, and the received signal at $R1$ is given by:

$$y_{R_1}(t) = h_{SR_1} s_0(t) + n_1(t), \quad (8)$$

where h_{SR_1} is the channel gain from S to $R1$. $n_1(t)$ is the noise at $R1$, which can be considered as a combination of the ambient light, thermal, dark, and shot noise of the Rx, modeled as an additive white Gaussian noise (AWGN) with zero mean and a power spectral density of N_0 [1]. $y_{R_1}(t)$ is afterwards amplified using an optical amplifier (OA) and then retransmitted to $R2$ via the second free space turbulence channel. The received signal at $R2$ is given as:

$$y_{R_2}(t) = h_{R_1R_2}(g_1 y_{R_1}(t) + a_1(t)) + n_2(t), \quad (9)$$

where a_1 is the amplified spontaneous emission (ASE) noise of OA at $R1$ and $n_2(t)$ is the noise at $R2$. In most previous works reported on relay-assisted FSO networks, the OA gain g was assumed to be fixed [15], [19], [20], [22], [34]. However, in this work we define g_j for jth OA relay (j = 1, 2, 3) as [24]:

$$g_j = \sqrt{\frac{P_{R_j}}{h_{j-1,j}^2 P_S^2 + N_0}}, \quad (10)$$

where P_s and P_R are the transmit and received powers at S and relay/destination (i.e., either $R1$, $R2$, or D), respectively. Note that, we assume that the relay transmits the signal under a maximum total power constraint and g is self-adjusted in order to ensure a fixed output power with varying input powers, which is typical for real optical networks comparable to theoretical works based on assumptions from RF domain. At D, the received signal prior to amplification is given as:

$$y_D(t) = h_{R_2D}(g_2 y_{R_2}(t) + a_2(t)) + n_3(t), \quad (11)$$

where a_2 is the ASE noise of OA at $R2$ and n_3 is the noise at D. Following pre-amplification at the Rx the signal is given as:

$$y_D'(t) = g_3 y_D(t) + a_3(t), \quad (12)$$

where a_3 is the ASE noise of OA at $R3$. Similarly, (12) can be written as:

$$y_D'(t) = g_1 g_2 g_3 h_{R_1R_2} h_{R_2D}[h_{SR_1} s_0(t) + n_1(t)] + g_2 g_3 h_{R_2D}[h_{R_1R_2} a_1(t) + n_2(t)] + g_3[h_{R_2D} a_2(t) + n_3(t)] + a_3(t). \quad (13)$$

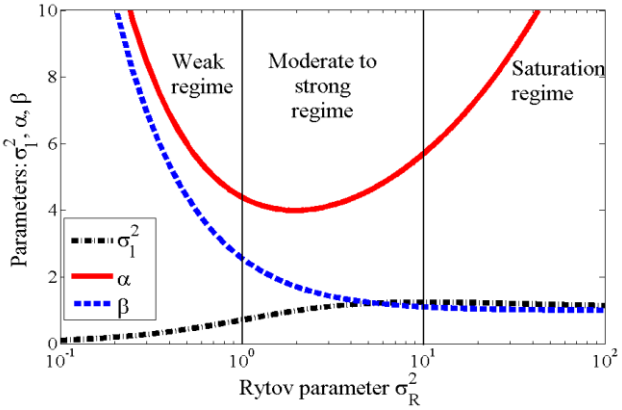

Fig. 2: Values of σ_I^2, α, and β under different turbulence regimes: weak, moderate to strong, and saturation

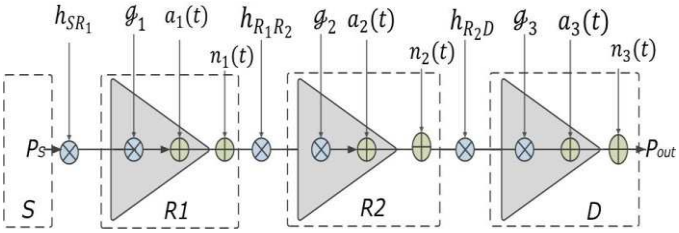

Fig. 3: Schematic block diagram of a triple-hop all-optical AF relay-assisted FSO link.

This article has been accepted for publication in a future issue of this journal, but has not been fully edited. Content may change prior to final publication. Citation information: DOI 10.1109/JLT.2016.2629081, Journal of Lightwave Technology

III. Performance Analysis

In this section, we derive the analytical SNR and BER for the triple-hop AF all-optical FSO link over the ΓΓ turbulence channel as end-to-end performance indicators. From (13), we can consider $y_D'(t)$ to be equivalent to a direct transmission system whose input-output relation is represented by:

$$y_D'(t) = h_{eq}s_0(t) + n_{eq}, \tag{14}$$

where $h_{eq} = g_1 g_2 g_3 h_{SR_1} h_{R_1R_2} h_{R_2D}$ and n_{eq} is the AWGN with zero mean and variance σ^2 given by:

$$\sigma^2 = \frac{g_1^2 g_2^2 g_3^2 \sigma_{n_1}^2 + g_2^2 g_3^2 \sigma_{a_1}^2 + g_2^2 g_3^2 \sigma_{n_2}^2 + g_3^2 \sigma_{a_2}^2 + g_3^2 \sigma_{n_3}^2 + \sigma_{a_3}^2}{g_1^2 g_2^2 g_3^2 + 2 g_2^2 g_3^2 + 2 g_3^2 + 1}. \tag{15}$$

In (15), we have used the fact that $E\left[h_{SR_1}^2\right]$, $E\left[h_{R_1R_2}^2\right]$, and $E\left[h_{R_2D}^2\right]$ of ΓΓ distribution are equal to 1. Thus, the end-to-end SNR γ_{e2e}, of the overall system can be written as:

$$\gamma_{e2e} = \frac{(g_1 g_2 g_3 h_{SR_1} h_{R_1R_2} h_{R_2D})^2}{\psi}, \tag{16a}$$

where

$$\psi = g_2^2 g_3^2 h_{R_2D}^2 \left(g_1^2 h_{R_1R_2} \sigma_{n_1}^2 + \sigma_{a_1}^2\right) + g_3^2 h_{R_2D}^2 \left[g_2^2 \sigma_{n_2}^2 + \sigma_{a_2}^2\right) + g_3^2 \sigma_{n_3}^2 + \sigma_{a_3}^2. \tag{16b}$$

In order to compute the BER, we have used the PDF derivation of a product of two random variables (RVs), which is generally given as [35]:

$$f(z) = \int_{-\infty}^{\infty} \frac{1}{|x|} f_X(x) f_Y\left(\frac{z}{x}\right) dx, \tag{17}$$

where z is the product of RVs x and y ($z = xy$). Using (17) and the concept of transformation of RVs, we can derive the PDF of h_{eq} in Meijer-G function as:

$$f\left(h_{eq}\right) = \left(\frac{(\alpha\beta)^{\frac{\alpha+\beta}{2}}}{\Gamma(\alpha)\Gamma(\beta)}\right)^3 \frac{h_{eq}^{\frac{\alpha+\beta}{2}-1}}{(g_1 g_2 g_3)^{\frac{\alpha+\beta}{2}}} \times G_{0,6}^{6,0}\left(\frac{(\alpha\beta)^3 h_{eq}}{g_1 g_2 g_3}\middle| \begin{matrix} -,- \\ \frac{\alpha-\beta}{2}, \frac{\beta-\alpha}{2}, \frac{\alpha-\beta}{2}, \frac{\beta-\alpha}{2}, \frac{\alpha-\beta}{2}, \frac{\beta-\alpha}{2} \end{matrix}\right). \tag{18}$$

Following this, the CDF of the h_{eq} is evaluated as:

$$F\left(h_{eq}\right) = \left(\frac{(\alpha\beta)^{\frac{\alpha+\beta}{2}}}{\Gamma(\alpha)\Gamma(\beta)}\right)^3 \left(\frac{h_{eq}}{g_1 g_2 g_3}\right)^{\frac{\alpha+\beta}{2}} \times G_{1,7}^{6,1}\left(\frac{(\alpha\beta)^3 h_{eq}}{g_1 g_2 g_3}\middle| \begin{matrix} \frac{2-\alpha-\beta}{2} \\ \frac{\alpha-\beta}{2}, \frac{\beta-\alpha}{2}, \frac{\alpha-\beta}{2}, \frac{\beta-\alpha}{2}, \frac{\alpha-\beta}{2}, \frac{\beta-\alpha}{2}, \frac{-\alpha-\beta}{2} \end{matrix}\right). \tag{19}$$

Considering the non-return-to-zero on-off keying (NRZ OOK) modulated signal format, the probability of error as a function of h_{eq} is given by:

$$P_e\left(h_{eq}\right) = \frac{1}{2} erfc\left(\frac{h_{eq}}{2\sqrt{2\sigma^2}}\right). \tag{20}$$

Therefore, the BER can be obtained from [20] as:

$$P_e = -\int_0^{\infty} F\left(h_{eq}\right) dP_e\left(h_{eq}\right). \tag{21}$$

From (A5) in Appendix A and CDF of h, the BER of the dual-hop system can be written as:

$$P_{e2} = \left(\frac{(\alpha\beta)^{\frac{\alpha+\beta}{2}}}{\Gamma(\alpha)\Gamma(\beta)}\right)^2 \frac{(8\sigma_2^2)^{\frac{\alpha+\beta+2}{4}}}{4\sqrt{2\pi\sigma_2^2}(g_1 g_2)^{\frac{\alpha+\beta}{2}} 2^2 (2\pi)^2} \times G_{3,10}^{8,3}\left(\frac{8\sigma_N^2(\alpha\beta)^4}{2^8 g_1^1 g_2^2}\middle| \begin{matrix} \frac{2-\alpha-\beta}{4}, \frac{2-\alpha-\beta}{4}, \frac{4-\alpha-\beta}{4} \\ \mathcal{G}^2, \frac{-\alpha-\beta}{4}, \frac{2-\alpha-\beta}{4} \end{matrix}\right), \tag{22}$$

where $= \frac{\alpha-\beta}{4}, \frac{\alpha-\beta+2}{4}, \frac{\beta-\alpha}{4}, \frac{\beta-\alpha+2}{4}$. Similarly, the BER for a triple-hop system is given as follows:

$$P_{e3} = \left(\frac{(\alpha\beta)^{\frac{\alpha+\beta}{2}}}{\Gamma(\alpha)\Gamma(\beta)}\right)^3 \frac{(8\sigma^2)^{\frac{\alpha+\beta+2}{4}}}{4\sqrt{2\pi\sigma^2}(g_1 g_2 g_3)^{\frac{\alpha+\beta}{2}} 8(2\pi)^3} \times G_{3,14}^{12,3}\left(\frac{8\sigma^2(\alpha\beta)^6}{2^{12}(g_1 g_2 g_3)^2}\middle| \begin{matrix} \frac{2-\alpha-\beta}{4}, \frac{2-\alpha-\beta}{4}, \frac{4-\alpha-\beta}{4} \\ \frac{\alpha-\beta}{4}, \frac{\alpha-\beta+2}{4}, \frac{\beta-\alpha}{4}, \frac{\beta-\alpha+2}{4}, \frac{\alpha-\beta}{4}, \frac{\alpha-\beta+2}{4}, \frac{\beta-\alpha}{4}, \frac{\beta-\alpha+2}{4}, \\ \frac{\alpha-\beta}{4}, \frac{\alpha-\beta+2}{4}, \frac{\beta-\alpha}{4}, \frac{\beta-\alpha+2}{4}, \frac{-\alpha-\beta}{4}, \frac{2-\alpha-\beta}{4} \end{matrix}\right). \tag{23}$$

By carefully observing (22) and (23), we can further generalize the BER expression for N-hop link as:

$$P_e = \left(\frac{(\alpha\beta)^{\frac{\alpha+\beta}{2}}}{\Gamma(\alpha)\Gamma(\beta)}\right)^N \frac{(8\sigma^2)^{\frac{\alpha+\beta+2}{4}}}{4\sqrt{2\pi\sigma_N^2}(g_N)^{\frac{\alpha+\beta}{2}} 2^N (2\pi)^N} \times G_{3,4N+2}^{4N,3}\left(\frac{8\sigma_N^2(\alpha\beta)^{2N}}{2^{4N}\mathcal{F}_N^2}\middle| \begin{matrix} \frac{2-\alpha-\beta}{4}, \frac{2-\alpha-\beta}{4}, \frac{4-\alpha-\beta}{4} \\ \mathcal{G}^N, \frac{-\alpha-\beta}{4}, \frac{2-\alpha-\beta}{4} \end{matrix}\right), \tag{24}$$

where $\mathcal{F}_N = g_1 g_2 \ldots g_N$, $\mathcal{G}^N$ implies that $\mathcal{G}$ is repeated N-times, and σ_N^2 denotes the equivalent variance for N-hop. Note that, if we consider the value of all gains to be equal as g then $\mathcal{F} = g^N$.

IV. Experimental Setup

With the outdoor FSO measuring set-up developed it is challenging and time consuming to carry out full system performance evaluation under all weather conditions. However, using the purpose built indoor laboratory testbed we are able to carry out comprehensive measurement campagin for the proposed system under a controlled environment over a short time scale. The schematic diagrams of proposed indoor experimental single, dual-hop, and triple-hop AF FSO relay assisted systems setup are illustrated in Figs. 4(a), (b), and (c), respectively. The systems are composed of a combination of FSO links of a total span of 6.6 m, EDFA, single mode fibers (SMF), and optical components. Note that, the experimental campaign took three weeks to be completed where we carried out several measurements for each turbulence regimes to ensure repeatability of results. As shown in Fig. 4(a), at the Tx, a signal source/BER tester (BERT-VeEX VEPAL TX300) is used to generate a pseudo-random binary sequence (PRBS) d_i in the NRZ-OOK format at R_d of 10 Gbps for IM of a 1550 nm distributed feedback (DFB) laser diode. An optical digital attenuator and a 50/50 coupler are used to control the level of transmit power P_s and split the signal into two, for both transmission and monitoring using an optical spectrum analyzer (OSA). The laser output is then launched into the free space channel via a gradient-index (GRIN) fiber collimator (Thorlabs 50-1550A-APC) with a clear aperture diameter lens of 0.18 cm. In order to focus the optical beam and minimize the divergence of the optical beam, two plano convex lenses Lens 1 and Lens 2 with a focal length f of 10 cm were placed after the Tx and before the Rx, respectively. At the Rx a GRIN fiber collimator is used to couple the received optical beam into the SMF the output of which is amplified using an EDFA. The signal is then applied via a 50/50 coupler to an OSA and a BERT for the link assessment in terms of the BER and SNR. Both dual-hop and a triple-hop AF FSO relay system were implemented based on Fig. 4(a). Fig. 5 depicts

This article has been accepted for publication in a future issue of this journal, but has not been fully edited. Content may change prior to final publication. Citation information: DOI 10.1109/JLT.2016.2629081, Journal of Lightwave Technology

the photo of an indoor experimental setup for the triple-hop AF FSO link as shown in Fig. 4(c).

In a controlled indoor environment using a dedicated atmospheric chamber, the strength of turbulence is controlled by blowing hot air from two 2 kW external heating fans in the direction perpendicular to the propagating optical beam along the transmission path. The heating sources were positioned near and/or away from the FSO Tx or Rx as shown in Fig. 5. In order to maintain a constant temperature gradient within the chamber well above the required 6 °C along the propagation path the temperature were kept at the room temperature of ~25 °C and within the range of 25 °C to 80 °C, respectively with the wind speed of <10 m/s. The strength of turbulence was varied by means of controlling the output of the fan heaters and thus varying the temperature profile. Moreover, two plastic barriers were placed at the ends of optical table in order to maintain the temperature profile along the chamber. To continuously monitor the temperature profile along the channel and ultimately be able to determine C_n^2, we recorded the instantaneous temperatures every 4 seconds throughout the experiment using 20 temperature sensors positioned at 0.28 cm apart along the channel (i.e., between the Tx and the Rx). While carrying out the experimental measurement with no turbulence, we ensured that the temperature along the channel was kept at the room temperature. With turbulence, we continuously recorded the temperature at 20 different positions T_1-T_{20} along the channel. All the main parameters adopted in the experimental setup are summarized in Table 1.

V. Results and Discussions

In this section, the experimental results for the single, dual-hop, and triple-hop all-optical FSO relay-assisted systems with and without turbulence are presented. The relays are located at equal distance between *S* and *D* in order to ensure that FSO links were balanced and SNR was the same for each hop. Based on the measured temperature profile and the calculation using (5), (6) and (7), we have determined three average values of the turbulence C_n^2 of 3.8×10^{-10} m$^{-2/3}$, 5.5×10^{-11} m$^{-2/3}$, and 5.4×10^{-12} m$^{-2/3}$ corresponding to σ_R^2 of 0.77, 0.11, and 0.01, respectively for total link span of 6.6 m. Results are validated theoretically by means of numerical evaluation of the BER using (22).

Fig. 6(a) presents comparison of measured and theoretical BER performance for single, dual, and triple-hop FSO links under a clear channel with no turbulence. We can observe from the figure that with the serial relay-assisted technique there is a remarkable improvement in the BER performance compared to the link with no relays. For example, for the measured data, at a BER of 10^{-5} there are ~3.0 dB and ~6.0 dB of SNR gains for dual and triple-hops, respectively compared to the single FSO link. Note that, by splitting the overall link span into smaller sections more energy (or power) is conserved. Notice the perfect match between theoretical and measured plots for all cases, particularly for the BER range below 10^{-4}. The slight mismatch between predicted and measured plots at higher values of BER (i.e., >10^{-4}) is due to losses associated with the optical components and ASE noise of EDFA in experimental case.

Fig. 6(b) then illustrates the measured and predicted BER performance against the SNR for single, dual, and triple-hop FSO links under a turbulence regime (i.e., $C_n^2 = 3.8 \times 10^{-10}$ m$^{-2/3}$) compared with the experimental result for the triple-hop link with no turbulence. As expected, under a stronger turbulence regime the propagating optical wave front will

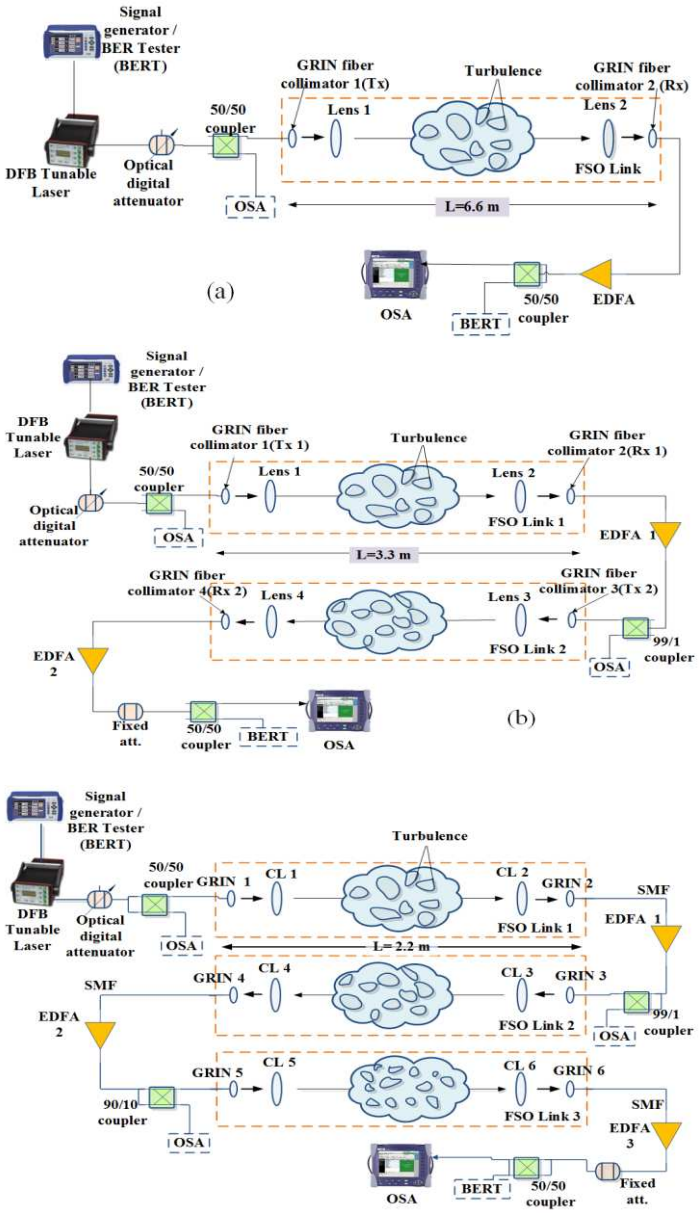

Fig. 4: Block diagram of the experimental setup of (a) direct link (b) dual-hop (c) triple-hop AF FSO relay-assisted systems

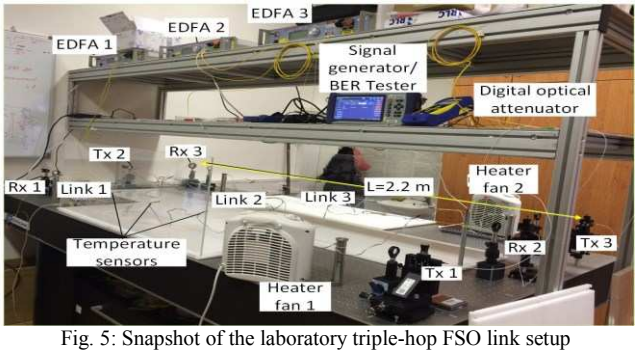

Fig. 5: Snapshot of the laboratory triple-hop FSO link setup

This article has been accepted for publication in a future issue of this journal, but has not been fully edited. Content may change prior to final publication. Citation information: DOI 10.1109/JLT.2016.2629081, Journal of Lightwave Technology

TABLE I
MAIN PARAMETERS USED IN EXPERIMENT

	Parameter	Value
Transmitter	Data rate and signaling scheme	10 Gbps NRZ-OOK
	Laser type	DFB
	Wavelength	1550 nm
	Output power	0.91 dBm
	Grin-lens aperture	0.18 cm
	Beam divergence	0.25 mrad
Lens	Clear aperture	2.54 cm
	Focal distance	10 cm
EDFA	Max. output power	21 dBm
	Noise figure	< 7.5 dB
Receiver	Clear aperture	0.18 cm
	Detector type	PIN
	Receiver sensitivity	-16 to -1 dBm
	Responsivity	0.6
SMF-28	Mode field diameter @ 1550 nm	10.4 ± 0.8 μm
	Attenuation @ 1550 nm	≤ 0.2 dB/km

experience much higher degree of intensity and phase fluctuations [21]. Similar to Fig. 6 (a), we observe that the relay-assisted schemes offer much improved BER performance compared to the direct FSO link. For example, at a target BER of 10^{-5}, (well below the forward error correction standard of 10^{-3}) the SNR gains are ~1.5 dB and ~4.2 dB for dual-hop and triple-hop links, respectively for the measured data when compared to the direct FSO link experiencing the same level of turbulence. These higher performance gains are because of the ability of multi-hop transmissions to exploit the distance-dependent TIF variance. Comparing the predicted with experimental results confirms the validity of the BER analysis outlined in Section III. Note that, at a BER of 10^{-5} the SNR penalty for the triple-hop link with turbulence is ~4 dB when compare to the same link without turbulence. This additional SNR is required to compensate for the turbulence induced power fades.

Furthermore, Fig. 6(c) depicts the experimental and theoretical results for the BER performance against the SNR for single, dual-hop, and triple-hop FSO links for $C_n^2 = 5.4 \times 10^{-12}$ $m^{-2/3}$. As a benchmark, the measured BER of a triple-hop link with no turbulence is also shown in the figure. By increasing the number of hops/relays, there is an improvement in the SNR requirement. The results confirm the potential of the relaying system in combating the TIF compared to the direct single link. As observed, there is a trade-off between the number of relays and the average P_s to achieve a particular BER. For example, for measured plots at a BER of10^{-5} the SNR gains are ~2.8 dB and ~4.8 dB for dual-hop and triple-hop, respectively compared to the single FSO link. As mentioned before, these SNR gains are because of reduced effects of the turbulence as the link span is shortened in relayed based systems. The marginal differences between the theoretical and measured plots in terms of SNR less than 0.5 dB at higher values of BER stem from the fact that no ideal theoretical turbulence flow can be experienced in real practical environment. Furthermore, at a BER of 10^{-5} and $C_n^2 = 5.4 \times 10^{-12}$ $m^{-2/3}$, the SNR penalty for the triple-hop link is ~2.0 dB compare to link with no turbulence. The SNR penalty is approximately 2.0 dB less compared to the link with $C_n^2 = 3.8 \times 10^{-10}$ $m^{-2/3}$ as in Fig. 6(c).

Moreover, Fig. 6(d) illustrates the measured and theoretical BER performance against the SNR for the case of triple-hop FSO link for different turbulence levels. We can observe reasonable match between the analytically simulated and measured plots. However, for lower values of SNR, the analytical results slightly differ from the measured data owing to the optical amplifier noise. The BER performance degrades with the turbulence strength. For example, at a BER of 10^{-5} the SNR penalties are ~ 2.0 dB, 3.7 dB, and ~4.0 dB for C_n^2 of 5.4×10^{-12} $m^{-2/3}$, 5.5×10^{-11} $m^{-2/3}$, and 3.8×10^{-10} $m^{-2/3}$, respectively compared to the link with no turbulence. Note at higher levels of turbulence the beam front of propagating optical wave experiences higher level of intensity and phase fluctuations, which ultimately leads to much wider, scattered and random optical beam patters at the Rx as discussed in [29]. This characteristic is best described by Kolmogrov's theory of turbulence where the refractive index changes in the order of several parts per million in every 1°K variation in the atmospheric temperature [32].

Finally, in order to provide more insight into the practical application of the system, we further consider the extension of the link span to 500 m, which is compatible with the last mile network access typical requirements in urban areas [1]. Fig. 7 shows the simulated BER performance for single, dual-hop, and triple-hop all-optical relay-assisted FSO links for C_n^2 of 10^{-12} and 10^{-16} $m^{-2/3}$, representing typical strong and weak turbulence regimes in an outdoor environment [36]. The plots confirm that the proposed scheme can successfully be adopted in a real practical environment, to ensure link availability and quality performance under turbulence conditions. For example, at a target BER of 10^{-3} the triple-hop link offers SNR gains of ~4 dB and ~5 dB for $C_n^2 = 10^{-16}$ and 10^{-12} $m^{-2/3}$, respectively, compared to the single link transmission case.

VI. CONCLUSIONS

In this paper, we investigated the performance of all-optical single, dual and triple-hop FSO links using the AF relaying technique over a turbulence channel. We carried out BER analysis for the general multi-hop relay-assisted FSO link considering the ΓΓ turbulence model, and validated them for the case of a triple-hop link through experiments. To the best of the authors' knowledge, this was the first experimental demonstration based on all-optical multiple-hop relay-assisted system. Results presented demonstrated a good agreement between the analytical calculations and measurements, particularly at relatively high SNRs. Based on the experimental results specifically, it was shown that the triple-hop FSO link substantially improves the overall link performance under atmospheric turbulence. Particularly, at a target BER of 10^{-5} about 4.8 dB and 4.2 dB of SNR gains were achieved compared to direct transmission for C_n^2 of 3.8×10^{-10} $m^{-2/3}$ and 5.4×10^{-12} $m^{-2/3}$, respectively. As it was analytically shown, these significant performance gains are due to the ability of multi-hop transmissions to exploit distance-dependent TIF variance by implicitly shortening the transmission span. By implementing an all-optical system, the overall system complexity is reduced (compared to electrical

This article has been accepted for publication in a future issue of this journal, but has not been fully edited. Content may change prior to final publication. Citation information: DOI 10.1109/JLT.2016.2629081, Journal of Lightwave Technology

relaying) making it an attractive solution for future ad-hoc optical wireless systems.

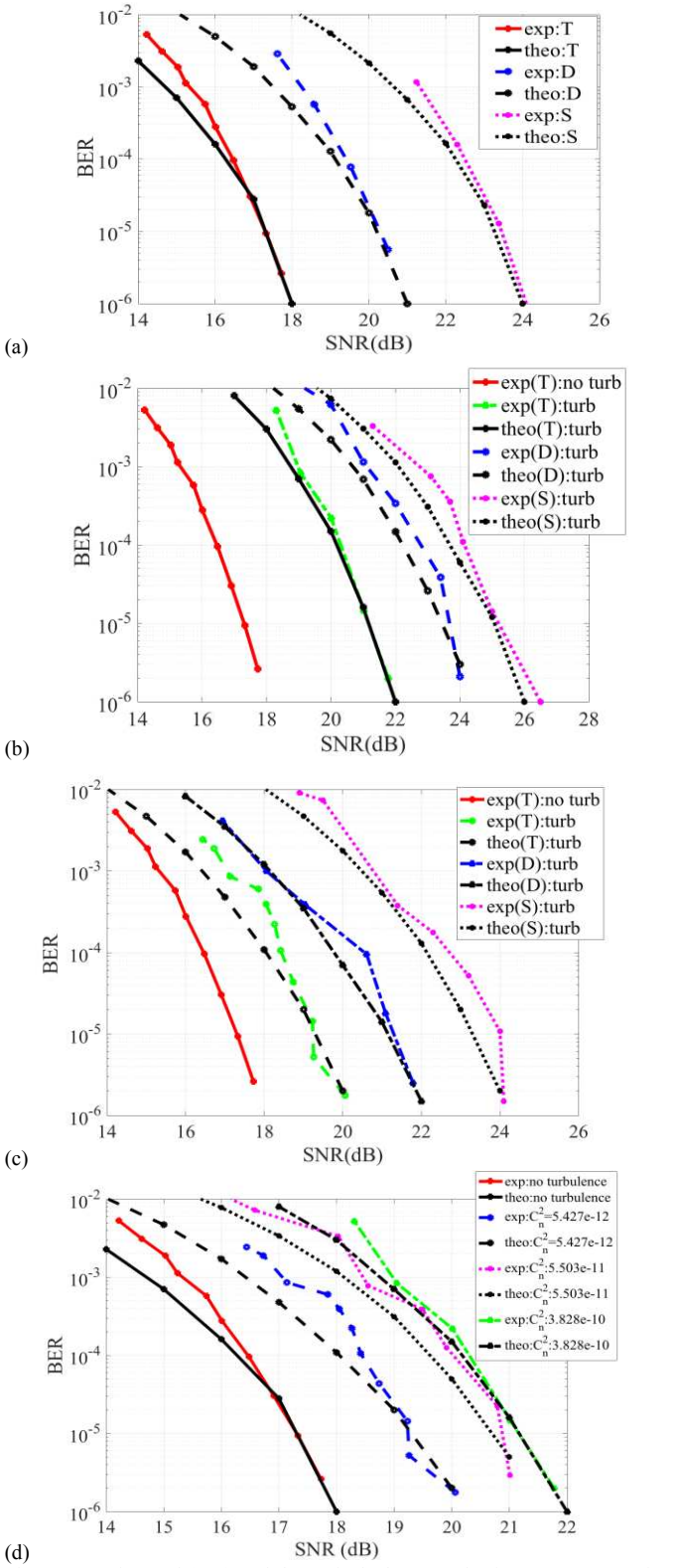

Fig. 6: Experimental (exp) and theoretical (theo) results for BER vs SNR for: (a) single (S), dual-hop (D), and triple-hop (T) with no turbulence; (b) S, D, T for $C_n^2 = 3.8 \times 10^{-10}$ m$^{-2/3}$, and exp. T with no turbulence (c) S, D, T links for $C_n^2 = 5.4 \times 10^{-12}$ m$^{-2/3}$, and an exp. T link with no turbulence; and (d) triple-hop link with and without turbulence.

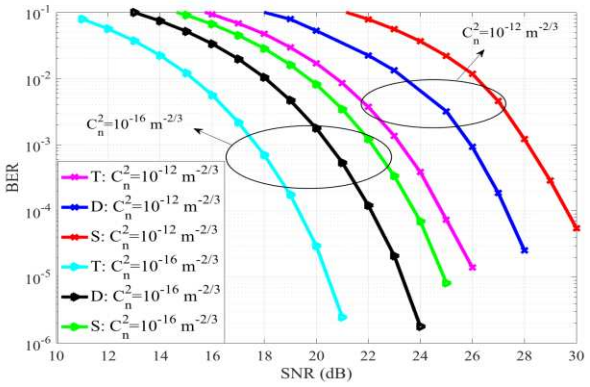

Fig. 7: Simulated BER performance for all-optical single (S), dual-hop (D), and triple-hop (T) FSO links for C_n^2 of 10^{-12} m$^{-2/3}$ and 10^{-16} m$^{-2/3}$ and a total link span of 500 m

APPENDIX A

The steps for the derivation of (18) using (17) are outlined below. From (1) we can write the PDF expressions for the channel gains of the source to $R1$ (h_{SR_1}) and $R1$ to $R2$ ($h_{R_1R_2}$), which are given as:

$$f(h_{SR_1}) = \frac{2(\alpha\beta)^{\frac{\alpha+\beta}{2}}}{\Gamma(\alpha)\Gamma(\beta)} (h_{SR_1})^{\frac{\alpha+\beta}{2}} K_{\alpha-\beta}\left(2\sqrt{\alpha\beta h_{SR_1}}\right), \quad \text{(A1)}$$

$$f(h_{R_1R_2}) = \frac{2(\alpha\beta)^{\frac{\alpha+\beta}{2}}}{\Gamma(\alpha)\Gamma(\beta)} (h_{R_1R_2})^{\frac{\alpha+\beta}{2}} K_{\alpha-\beta}\left(2\sqrt{\alpha\beta h_{R_1R_2}}\right). \quad \text{(A2)}$$

Using (17), and considering $h = h_{SR_1} h_{R_1R_2}$, the PDF of h can be computed as:

$$f(h) = \int_0^\infty f(h_{SR_1}) f\left(\frac{h}{h_{SR_1}}\right) \frac{1}{|h_{SR_1}|} dh_{SR_1}. \quad \text{(A3)}$$

Substituting the values from (22) and (23) and using the Meijer-G representation of the modified Bessel function of second type [[37], Eq.8.4.23.1] we can rewrite (A3) as:

$$f(h) = \left(\frac{(\alpha\beta)^{\frac{\alpha+\beta}{2}}}{\Gamma(\alpha)\Gamma(\beta)}\right)^2 h^{\frac{\alpha+\beta}{2}-1} \int_0^\infty h_{SR_1}^{-1} G_{0,2}^{2,0}\left(\alpha\beta h_{SR_1} \middle| \begin{matrix} -,- \\ \frac{\alpha-\beta}{2}, \frac{\beta-\alpha}{2} \end{matrix}\right) \times G_{0,2}^{2,0}\left(\frac{\alpha\beta h}{h_{SR_1}} \middle| \begin{matrix} -,- \\ \frac{\alpha-\beta}{2}, \frac{\beta-\alpha}{2} \end{matrix}\right) dh_{SR_1}. \quad \text{(A4)}$$

Using [[37], Eq. 8.24.1.1] and the property of Meijer-G function [[37], Eq. 8.2.2.15], we can obtain the PDF of h, which is given as:

$$f(h) = \left(\frac{(\alpha\beta)^{\frac{\alpha+\beta}{2}}}{\Gamma(\alpha)\Gamma(\beta)}\right)^2 \frac{h^{\frac{\alpha+\beta}{2}-1}}{g_1^{\frac{\alpha+\beta}{2}}} G_{0,4}^{4,0}\left(\frac{(\alpha\beta)^2 h}{g_1} \middle| \begin{matrix} - \\ \frac{\alpha-\beta}{2}, \frac{\beta-\alpha}{2}, \frac{\alpha-\beta}{2}, \frac{\beta-\alpha}{2} \end{matrix}\right). \quad \text{(A5)}$$

Since the proposed system has three-hop, the PDF of the channel gain for $R2$ to D (h_{R_2D}), which is also ΓΓ distributed, can be expressed as in (A1) and (A2):

$$f(h_{R_2D}) = \frac{2(\alpha\beta)^{\frac{\alpha+\beta}{2}}}{\Gamma(\alpha)\Gamma(\beta)} (h_{R_2D})^{\frac{\alpha+\beta}{2}} K_{\alpha-\beta}\left(2\sqrt{\alpha\beta h_{R_2D}}\right). \quad \text{(A6)}$$

Now, let's consider a new random variable $h_{3e} = h h_{R_2D}$. Using (17) in the same way to derive $f(h)$, we obtain the PDF of the equivalent SNR at the destination as follow:

This article has been accepted for publication in a future issue of this journal, but has not been fully edited. Content may change prior to final publication. Citation information: DOI 10.1109/JLT.2016.2629081, Journal of Lightwave Technology

$$f(h_{3e}) = \left(\frac{(\alpha\beta)^{\frac{\alpha+\beta}{2}}}{\Gamma(\alpha)\Gamma(\beta)}\right)^3 \frac{h_{3e}^{\frac{\alpha+\beta}{2}-1}}{\mathcal{g}_1\mathcal{g}_2^{\frac{\alpha+\beta}{2}}} \times G_{0,6}^{6,0}\left(\frac{(\alpha\beta)^3 h_{3e}}{\mathcal{g}_1\mathcal{g}_2}\middle| \begin{matrix} - \\ \frac{\alpha-\beta}{2}, \frac{\beta-\alpha}{2}, \frac{\alpha-\beta}{2}, \frac{\beta-\alpha}{2}, \frac{\alpha-\beta}{2}, \frac{\beta-\alpha}{2} \end{matrix}\right) \quad \text{(A7)}$$

It can be seen from Fig. 3 that experimental setup uses one more amplifier gain. Following (18), the final PDF for the equivalent channel gain $h_{eq} = \mathcal{g}_3 h_{3e}$ for the given system is obtained as:

$$f(h_{eq}) = \left(\frac{(\alpha\beta)^{\frac{\alpha+\beta}{2}}}{\Gamma(\alpha)\Gamma(\beta)}\right)^3 \frac{h_{3e}^{\frac{\alpha+\beta}{2}-1}}{(\mathcal{g}_1\mathcal{g}_2\mathcal{g}_3)^{\frac{\alpha+\beta}{2}}} \times G_{0,6}^{6,0}\left(\frac{(\alpha\beta)^3 h_{eq}}{\mathcal{g}_1\mathcal{g}_2\mathcal{g}_3}\middle| \begin{matrix} - \\ \frac{\alpha-\beta}{2}, \frac{\beta-\alpha}{2}, \frac{\alpha-\beta}{2}, \frac{\beta-\alpha}{2}, \frac{\alpha-\beta}{2}, \frac{\beta-\alpha}{2} \end{matrix}\right) \quad \text{(A8)}$$

REFERENCES

[1] Z. Ghassemlooy, W. Popoola, and S. Rajbhandari, *Optical wireless communications: System and channel modelling with MATLAB*. United Kingdom: CRC Press Taylor and Francis Group, 2013.

[2] M. A. Khalighi and M. Uysal, "Survey on free space optical communication: A communication theory perspective," *IEEE Commun. Surv. Tutorials*, vol. 16, no. 4, pp. 2231–2258, 2014.

[3] A. Paraskevopoulos, J. Vucic, S. H. Voss, R. Swoboda, and K.-D. Langer, "Optical wireless communication systems in the Mb/s to Gb/s range, suitable for industrial applications," *IEEE/ASME Trans. Mechatronics*, vol. 15, no. 4, pp. 541–547, 2010.

[4] G. Parca, "Optical wireless transmission at 1.6-Tbit/s (16×100 Gbit/s) for next-generation convergent urban infrastructures," *Opt. Eng.*, vol. 52, no. 11, p. 116102, Nov. 2013.

[5] S. Bloom, E. Korevaar, and J. Schuster, "Understanding the performance of free-space optics [Invited]," *J. Opt. Netw.*, vol. 2, no. 6, pp. 178–200, 2003.

[6] L. C. Andrews and R. L. Phillips, *Laser beam propagation through random media*, 2nd Ed. Washington, USA: SPIE Press, 2005.

[7] Z. Zhao, S. D. Lyke, and M. C. Roggemann, "Adaptive optical communication through turbulent atmospheric channels," in *IEEE Int. Conf. on Commu.*, 2008, pp. 5432–5436.

[8] G. Yang, M.-A. Khalighi, Z. Ghassemlooy, and S. Bourennane, "Performance evaluation of receive-diversity free-space optical communications over correlated gamma-gamma fading channels," *Appl. Opt.*, vol. 52, no. 24, pp. 5903–11, Aug. 2013.

[9] M.-A. Khalighi, N. Schwartz, N. Aitamer, and S. Bourennane, "Fading reduction by aperture averaging and spatial diversity in optical wireless systems," *J. Opt. Commun. Netw.*, vol. 1, no. 6, pp. 580–593, Oct. 2009.

[10] W. O. Popoola, "Subcarrier intensity modulated free-space optical communication systems," Ph.D. thesis, School of Computing, Engineering. and Information Sciences, University of Northumbria at Newcastle, 2009.

[11] A. Andò, S. Mangione, L. Curcio, S. Stivala, G. Garbo, R. Pernice, and A. C. Busacca, "Recovery capabilities of rateless codes on simulated turbulent terrestrial free space optics channel model," *Int. J. Antennas Propag.*, vol. 2013, no. Article ID 692915, 2013.

[12] M. Ahmad and O. Awwad, "Synergies of radio frequency and free space optics communication : New hybrid solutions for next generation wireless mesh networks," *Int. J. Comput. Networks*, vol. 4, no. 4, pp. 135–155, 2012.

[13] S. Anees and M. R. Bhatnagar, "Performance of an amplify-and-forward dual-hop asymmetric RF–FSO communication system," *J. Opt. Commun. Networks*, vol. 7, no. 2, pp. 124–135, 2015.

[14] M. Uysal and M. M. Fareed, "Cooperative diversity systems for wireless communication," in *Sel. Topics in Inf. and Cod. Theo.*, World Scientific, 2010, pp. 623–662.

[15] M. Safari and M. Uysal, "Relay-assisted free-space optical communication," *IEEE Trans. Wirel. Commun.*, vol. 7, no. 12, pp. 5441–5449, 2008.

[16] M. Karimi and M. Nasiri-Kenari, "BER analysis of cooperative systems in free-space optical networks," *J. Lightw. Technol.*, vol. 27, no. 24, pp. 5639–5647, Dec. 2009.

[17] C. K. Datsikas, K. P. Peppas, N. C. Sagias, and G. S. Tombras, "Serial free-space optical relaying communications over gamma-gamma atmospheric turbulence channels," *J. Opt. Commun. Netw.*, vol. 2, no. 8, p. 576, Jul. 2010.

[18] M. R. Bhatnagar, "Performance analysis of decode-and-forward relaying in gamma-gamma fading channels," *IEEE Photonics Technol. Lett.*, vol. 25, no. 22, pp. 2197–2200, 2013.

[19] M. Karimi and M. Nasiri-kenari, "Free space optical communications via optical amplify-and-forward relaying," *J. Lightw. Technol.*, vol. 29, no. 2, pp. 242–248, 2011.

[20] S. Kazemlou, S. Hranilovic, and S. Kumar, "All-optical multihop free-space optical communication systems," *J. Lightw. Technol.*, vol. 29, no. 18, pp. 2663–2669, Sep. 2011.

[21] E. Bayaki, D. S. Michalopoulos, and R. Schober, "EDFA-based all-optical relaying in free-space optical systems," *IEEE Trans. Commun.*, vol. 60, no. 12, pp. 3797–3807, Dec. 2012.

[22] M. A. Kashani, M. M. Rad, M. Safari, and M. Uysal, "All-optical amplify-and-forward relaying system for atmospheric channels," *IEEE Commun. Lett.*, vol. 16, no. 10, pp. 1684–1687, Oct. 2012.

[23] P. V. Trinh, A. T. Pham, H. T. T. Pham, and N. T. Dang, "BER analysis of all-optical AF dual-hop FSO systems over gamma-gamma channels," *IEEE 4th Int. Conf. Photonics*, no. 1, pp. 175–177, Oct. 2013.

[24] L. Yang, X. Gao, and M. Alouini, "Performance analysis of relay-assisted all-optical FSO networks over strong atmospheric turbulence," *J. Lightw. Technol.*, vol. 32, no. 23, pp. 4011–4018, 2014.

[25] J. Zhang, L. Dai, Y. Zhang, and Z. Wang, "Unified performance analysis of mixed radio frequency/free space optical dual-hop transmission systems," *J. Lightw. Technol.*, vol. 33, no. 11, pp. 2286–2293, 2015.

[26] G. T. Djordjevic, M. I. Petkovic, A. M. Cvetkovic, and G. K. Karagiannidis, "Mixed RF/FSO relaying with outdated channel state information," *J. Sel. Areas Commun.*, vol. 33, no. 9, pp. 1935–1948, 2015.

[27] J. Libich, M. Komanec, S. Zvanovec, P. Pesek, W. O. Popoola, and Z. Ghassemlooy, "Experimental verification of all-optical dual hop 10 Gbit/s FSO link under turbulence regimes," *Opt. Lett.*, vol. 40, no. 3, pp. 391–394, 2015.

[28] N. A. M. Nor, J. Bohata, Z. Ghassemlooy, S. Zvanovec, P. Pesek, M. Komanec, and M. Khalighi, "10 Gbps all-optical relay-assisted FSO system over a turbulence channel," in *Int. Works. on Optical Wirel. Commu.*, 2015, pp. 1–4.

[29] Z. Ghassemlooy, H. Le Minh, S. Rajbhandari, J. Perez, and M. Ijaz, "Performance analysis of ethernet/fast-ethernet free space optical communications in a controlled weak turbulence conditions," *J. Lightw. Technol.*, vol. 30, no. 13, pp. 2188–2194, 2012.

[30] J. Perez, S. Zvanovec, Z. Ghassemlooy, and W. O. Popoola, "Experimental characterization and mitigation of turbulence induced signal fades within an ad hoc FSO network.," *Opt. Express*, vol. 22, no. 3, pp. 3208–18, 2014.

[31] M. Hulea, Z. Ghassemlooy, S. Rajbhandari, and X. Tang, "Compensating for optical beam scattering and wandering in FSO communications," *J. Lightw. Technol.*, vol. 37, no. 7, pp. 1323–1328, 2014.

[32] M. Amini Kashani, M. Uysal, and M. Kavehrad, "A novel statistical channel model for turbulence-induced fading in free-space optical systems," *J. Lightw. Technol.*, vol. 8724, no. 99, pp. 1–1, 2015.

[33] A. Majumdar and J. C. Ricklin, *Free-space laser communications: Principles and advances*. New York, USA: Springer, 2008.

[34] I. S. Ansari, F. Yilmaz, and M. S. Alouini, "Impact of pointing errors on the performance of mixed RF/FSO dual-hop transmission systems," *IEEE Wirel. Commun. Lett.*, vol. 2, no. 3, 2013.

[35] A. Papoulis and S. U. Pillai, *Probability, random variables, and stochastic processes*. New York: McGraw-Hill, 2002.

[36] M. A. Kallistratova and D. F. Timanovskiy, "The distribution of the structure constant of refractive index fluctuations in the atmospheric surface layer," *Repr. from Izv. Atmos. Ocean Phys.*, vol. 7, no. 1, pp. 73–75, 1990.

[37] A. P. Prudnikov, I. A. Brychkov, and O. I. Marichev, *Integrals and series: More special functions*, Vol 3. New York, USA: Gordon and Breach Science Publishers, 1990.